Chapter 4

Sliding Mode Control for Bidirectional Converter for G2V and V2G operations

4.1 Introduction

The increasing importance of BEVs in contemporary society is explored in this chapter. As an adequate replacement for conventional cars, BEVs are becoming increasingly popular on the roads due to their reduced carbon dioxide emissions. The heightened adoption of EVs is driving an increased need for power infrastructure. Additionally, EVs, functioning as portable power banks, can store substantial energy, making a noteworthy contribution to grid preservation and support [135]. As a consequence, the power electronics/systems research community has turned its attention to examining vehicle-to-X (V2X) technology. This groundbreaking approach enables the transfer of power from the vehicle's onboard battery to external infrastructure, as detailed in [136]. This chapter introduces the sliding mode control (SMC) applied to a DC/DC Bi-directional Power converter in a battery electric vehicle (BEV) charger. The primary objective is to track the desired output voltage and current of the charger precisely in both grid-to-vehicle (G2V) and vehicle-to-grid (V2G) modes [137]. BEV chargers facilitate efficient dual communication between the grid and vehicles in these configurations. However, managing power flow in

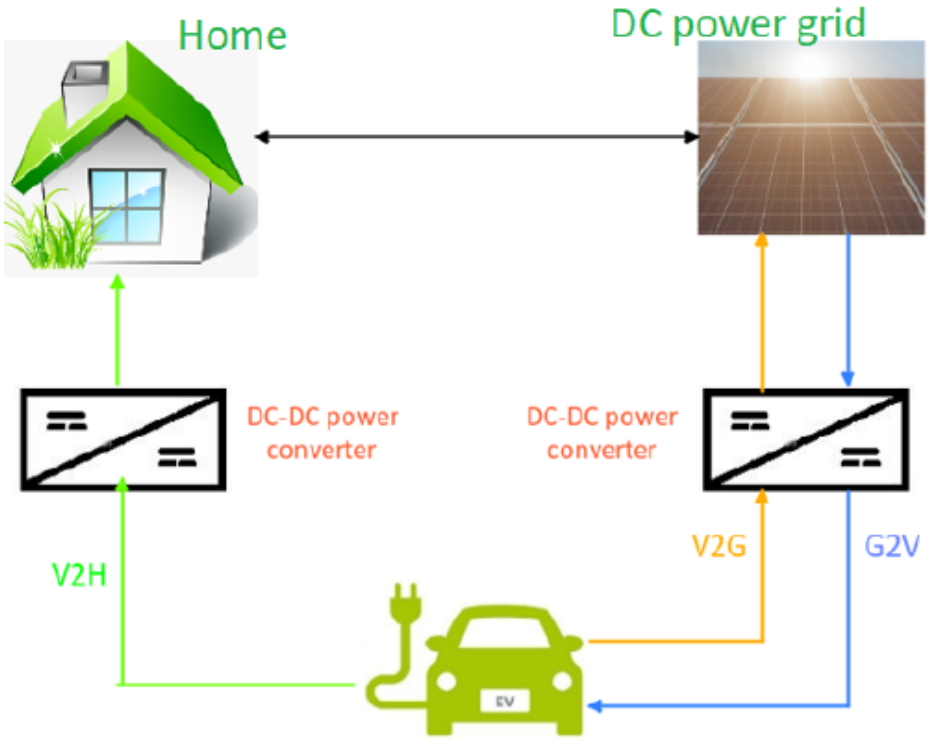

Figure 4.1: V2X technology schematic diagram with bidirectional DC/DC power converter.

either category poses challenges. SMC is proposed as a hardware-efficient solution for DC/DC converter control issues compared to existing PWM techniques [137]. Leveraging the increasing availability of commercially offered switching components, SMC regulates the converter's inner current loop, effectively reducing chattering effects and addressing significant drawbacks of power converters. The stability analysis of the converters is presented for both step-down and step-up operation modes. Simulation results demonstrate the efficacy of the proposed controller in both V2G and G2V modes [138, 139]. Consequently, the power electronics/systems research community has focused on examining vehicle-to-X (V2X) technology. This groundbreaking approach enables power transfer from the vehicle's onboard battery to external infrastructure, as detailed in [140].

This inventive strategy simplifies transferring power from the vehicle's onboard battery to external infrastructure, as elaborated in [138]. The practical utilization of V2X technology is projected to undergo considerable expansion in the foreseeable future. Fig. 4.1 depicts V2X technologies employing bidirectional DC-DC power

converters to enable power transfer from vehicles to different devices. This categorization includes V2L, V2H, V2G, and G2V modes [141].

4.2 Bi-directional Power Converters in EVs

This concept is behind developing bidirectional, highly effective, and inexpensive DC-DC conversion systems for V2G and V2H charging infrastructure in residential and commercial settings. V2G, V2H, and V2V technologies are all based on bidirectional DC/DC converters. Enabling EVs to feed energy back into the grid while parked and charging will improve grid resilience, facilitate greater use of renewable energy sources, and reduce the cost of ownership for EV owners. Through novel business opportunities, these benefits will accrue to EV users, consumers, and fleet managers. Fig. 4.1 illustrates a general block diagram of a Bi-directional DC/DC Power converter. Furthermore, many linear controllers have been proposed for BEV charging units, such as linear-quadratic controllers (LQC) and proportional-integral controllers (PI). So, the PI controller has proposed a SEPIC converter-based electric vehicle charger. These controllers can manage how the converter dynamics of BEV chargers operate. These controllers have better dynamic performance but only have one linearized working point and are not resistant to outside disturbances. The other important work on the controller design is to control the DC/DC Buck converter and the Boost converter's output voltage.

4.3 Bidirectional Power Flow Operations in EVs: G2V and V2G

A reliable infrastructure for charging EVs is essential. Two types of chargers use the grid's power supply, the battery: on-board and off-board chargers. Developing a dependable charging network is crucial for the advancement of EVs. EV chargers can be categorized into two primary types: conductive and inductive. Furthermore, EV chargers are classified as unidirectional and bidirectional based on how the power is transferred. Commonly, an EV charger includes two types of

converters: (i) a power factor correction AC/DC converter and (ii) battery integration using a DC/DC converter. These can only be performed in the G2V charging mode as they are usually unidirectional. However, to support V2X technologies, the converter needs to be bidirectional and have a high Power rating [139]. V2G technology uses the battery's vehicle to energize the grid, while the V2H technique uses the battery to power the house [142]. Bi-directional AC/DC converter operates in G2V mode just as a rectifier with sinusoidal current absorbance, and reversible type AC/DC converter performs as a buck converter. Similarly, An AC/DC converter provides inverting capability during V2G operating mode, but in reversible operation, DC/DC converter operates in boost mode [143]. Figs. 4.2 and 4.3 depict The general block diagram comprises a bidirectional DC-DC power converter and a bidirectional battery charger. Many researchers have utilized the SMC strategy to perform robustness analysis. As a nonlinear variable structure control method, SMC remains unaffected by uncertainty and parameter perturbations [144]. Power converter control is anticipated to use the SMC technique more frequently as the highest frequency of widely viable switching elements increases [145].

Based on the foregoing considerations and hardware limitations of PWM-based control, we are motivated to design the SMC for the Bi-directional DC/DC power converter of the BEV charger in G2V and V2G applications. This chapter's major contributions are as follows:

(i) A robust nonlinear sliding mode controller has been designed.

(ii) The system's dynamic response has been successfully attained, which is critical for improving the operational requirements of V2G and G2V.

(iii) In comparison to PWM-based control, this the approach provides easier hardware implementation.

4.4 Modeling and Sliding Mode Control of Power Converters

Modeling and Sliding Mode Control of power converters represent a critical domain in modern power electronics and control systems engineering. This field deals with

developing mathematical models to accurately describe the behavior of power converters, such as inverters, rectifiers, and DC-DC converters, and the design and implementation of control strategies to regulate their operation effectively.

Modeling of Power Converters: Power converters involve complex electrical and magnetic interactions. Mathematical models are developed to describe the voltage,

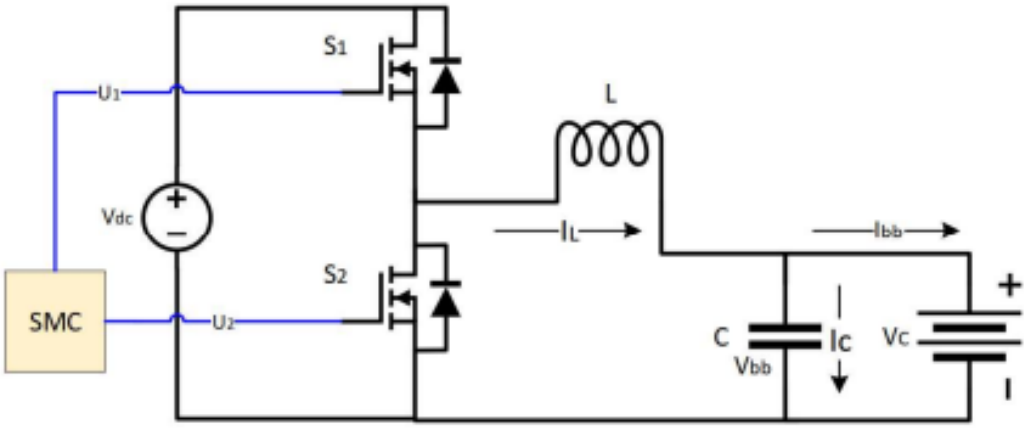

Figure 4.2: Control function block diagram of bidirectional DC-DC power converter.

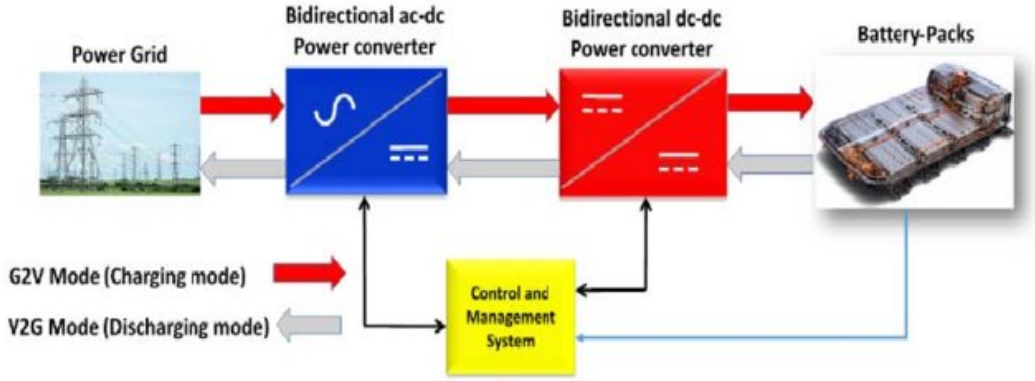

Figure 4.3: Block diagram of bidirectional Battery charger.

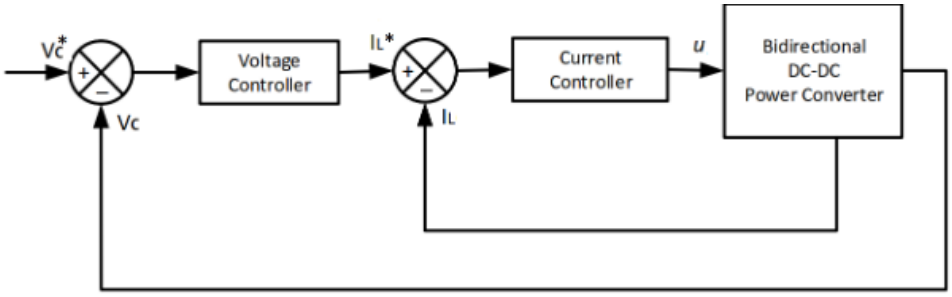

Figure 4.4: Block diagram of two-loop control.

current, and power transfer characteristics under different operating conditions.

Switching Dynamics Modeling: Power converters operate by rapidly switching semiconductor devices such as MOSFETs or IGBTs. Switching dynamics models capture the behavior of these devices during turn-on and turn-off transitions, including effects like voltage spikes and switching losses.

Control Loop Modeling: The control loops in power converters, including voltage and current control loops, must be modeled to analyze stability and performance. This involves describing the feedback mechanisms and their interactions with the converter dynamics.

Sliding Mode Control (SMC): SMC is a robust control technique that aims to drive the system state onto a predefined sliding surface, where the system dynamics become insensitive to uncertainties and disturbances.

Invariance to Parameter Variations: SMC is particularly attractive for power converters due to its inherent robustness against parameter variations, such as changes in load conditions or component tolerances.

Chattering Reduction: Chattering, a phenomenon associated with SMC, refers to high-frequency switching of control signals. Various techniques, such as boundary layer design and reaching law optimization, are employed to reduce chattering and improve control performance with Other control loops.

Applications: Renewable Energy Systems: Power converters are crucial in renewable energy systems such as solar photovoltaic and wind power generation. SMC techniques can enhance the performance and efficiency of these systems by ensuring reliable power conversion and grid integration.

Electric Vehicles: Power converters are essential components in electric vehicle propulsion systems and onboard chargers. SMC can provide robust control of traction inverters and improve the vehicle's dynamic response and energy efficiency.

Grid-Tied Converters: Power converters interfacing with the utility grid, such as grid-tied inverters in distributed energy systems, require precise control to regulate power flow and maintain grid stability. SMC can address challenges such as grid voltage fluctuations and load variations [146].

4.5 Electrical Architecture Description

This section proposes SMC for handling the nonlinear dynamics of BEV chargers and output voltage regulators and for tracking the reference voltages in V2G and G2V operating modes. So, this SMC regulates the converter's output voltage smoothly regardless of the mode of operation. DC/DC converters are typically characterized by fast and slow motion, with the fast motion driven by the input current dynamics and the slow motion driven by the dynamics of the output voltage. The cascaded control's structure is shown in Fig.4.4, with an outer and inner loop regulating output voltage and input current, respectively.

Fig. 4.5 illustrates the circuit schematic of a bidirectional DC-DC power converter, offering an overview of the electrical architecture employed in the system. Fig. 4.6 illustrates the equivalent circuit of the battery, offering a visual depiction of its components and how they are interconnected. The converter's two operating modes are depicted in Figs. 4.7 and 4.8. The step-down operation is illustrated in Fig. 4.7; the battery receives the electrical energy from the DC output link on the charger. The step-up operation is depicted in Fig. 4.8, and the DC output bus receives electricity from the battery. The step-down and step-up operations are examined in the next section to investigate the feasibility of a sliding-mode control law for this

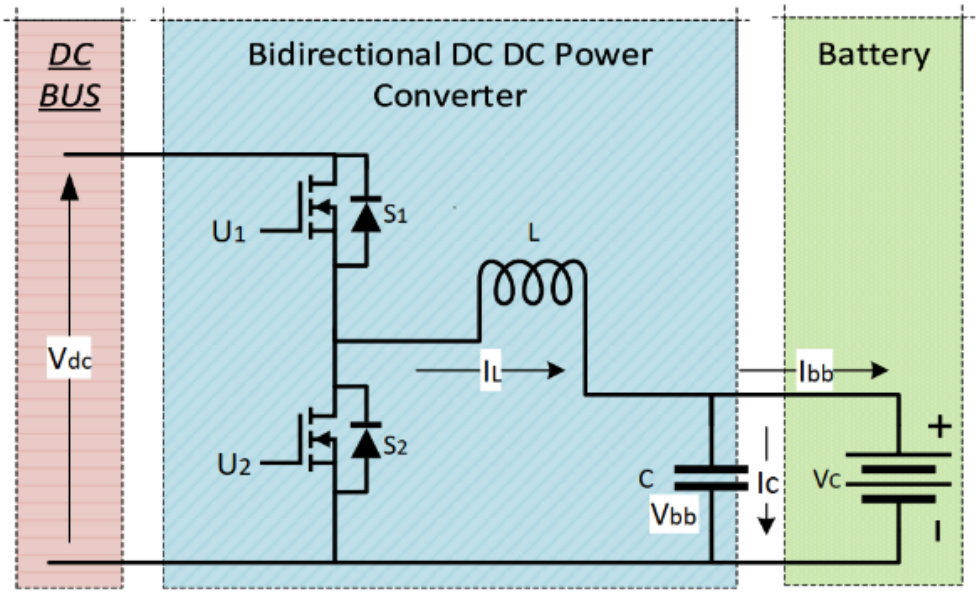

Figure 4.5: Bi-directional DC/DC Power converter circuit diagram.

bidirectional DC-DC power converter.

4.5.1 Current Control Loop Model

To regulate the inner current, the switching function can be described as follows:

$$s = I_L - I_{\text{ref}}. \tag{4.1}$$

To steer sliding mode in the manifold $s = 0$, the control u_i (taking only two values, 0 or 1) may be defined as follows:

$$u_i = \frac{1}{2}\left(1 - \text{sign(s)}\right), \quad i = 1, 2 \tag{4.2}$$

where u_1 is control for step-down mode and u_2 is control for step-up mode.

4.5.2 Step-down Mode

By using the step-down mode, the switch S_1 is controlled by a Sliding-Mode-based controller u_1, while switch S_2 remains open. The battery receives the electrical energy through the DC output link on the charger. This mode reduces the charger's output voltage to the battery's required level. G2V will be the mode of operation for the whole system. Fig. 4.7 presents the electrical circuit diagram of the converter, serving as the basis for deriving the subsequent switching model. The model is derived by employing the volt-second balance theorem and the charge-second balance

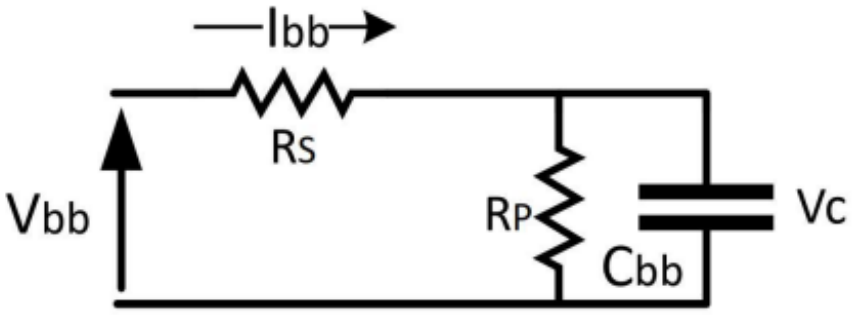

Figure 4.6: Battery equivalent circuit.

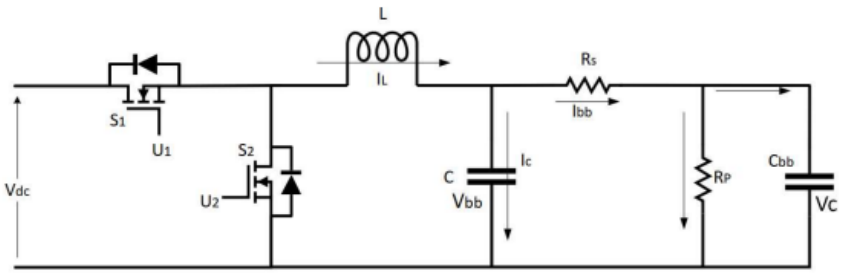

Figure 4.7: Circuit diagram of bidirectional DC/DC power converter in buck operating mode.

theorem.

$$\begin{cases} \frac{dI_L}{dt} & = \frac{-1}{L}V_{bb} + u_1\frac{V_{dc}}{L} \\ \frac{dV_{bb}}{dt} & = \frac{1}{C}I_L - \frac{1}{CR_s}V_{bb} + \frac{1}{CR_s}V_c \\ \frac{dV_c}{dt} & = \frac{1}{C_{bb}R_s}V_{bb} - \frac{1}{C_{bb}R_s}V_c - \frac{1}{C_{bb}R_p}V_c \end{cases} \tag{4.3}$$

The requirement for the existence of sliding mode is deduced from $s\dot{s} < 0$. Thus, the sliding mode exists if

$$0 < V_{bb} < V_{dc} \tag{4.4}$$

This above condition establishes the attraction domain of the Sliding Manifold. So, the domain of attraction (4.4) is set by the system architecture because the control (4.2) contains no control gain to be changed. The definition of a buck converter, which states that the output voltage is less than the source voltage, satisfies (4.2) in a steady state.

The sliding surface's motion is maintained by an equivalent control when the system reaches the sliding surface.

Invoking control scheme (4.2) and after solving $\dot{s} = \dfrac{dI_L}{dt} = 0$, the equivalent control $u_{1_{eq}}$ can be determined as

$$u_{1_{eq}} = \frac{V_{bb}}{V_{dc}}. \tag{4.5}$$

After that, the system's stability during step-down operation under sliding manifold

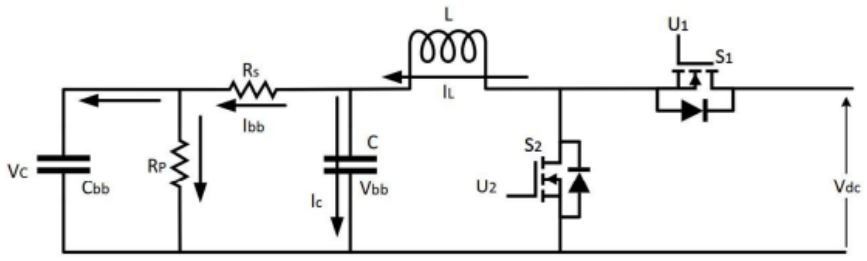

Figure 4.8: Circuit diagram of bidirectional DC/DC power converter in boost operating mode.

$s = 0$ is determined using the dynamic equations listed below

$$\frac{dI_L}{dt} = 0 \tag{4.6}$$

$$\frac{dV_{bb}}{dt} = \frac{u_{1_{eq}}}{C} I_{\text{ref}} - \frac{1}{CR_s} V_{bb} + \frac{1}{CR_s} V_c \tag{4.7}$$

$$\frac{dV_c}{dt} = \frac{1}{C_{bb}R_s} V_{bb} - \frac{1}{C_{bb}R_s} V_c - \frac{1}{C_{bb}R_p} V_c. \tag{4.8}$$

The above equations represent a 2^{nd}order system. The order is reduced by incorporating the sliding-mode current control, which controls I_L. Thus, the characteristic polynomial is calculated using the equations (4.7)-(4.8) as

$$P_{sd} = \frac{-1}{CC_{bb}R_sR_p} \left(\lambda^2 CC_{bb}R_sR_p + \lambda(CR_p + CR_s + C_{bb}R_p) + 1\right) \tag{4.9}$$

If both R_s and R_p are positive, the characteristic quadratic P_{sd} investigation has been demonstrated for a stable system. This criterion will always be met during the step-down mode so that the step-down mode will become stable.

4.5.3 Step-up Mode

This mode causes the sliding mode controller u_2 to control the switch S_2 while the switch S_1 remains open, i.e., equal to zero. The energy of the battery is transmitted to the DC bus. During this operation, this system is in V2G mode, and the DC/DC converter boosts the voltage to the desired level. Fig. 4.8 illustrates the corresponding electrical circuit for the converter. The following switching model can be obtained after applying the charge-second and volt-second balance theorems. We

can derive the following switching model:

$$\begin{cases} \frac{dI_L}{dt} & = \frac{1}{L}V_{bb} - (1-u_2)\frac{V_{dc}}{L} \\ \frac{dV_{bb}}{dt} & = -\frac{1}{C}I_L - \frac{1}{CR_s}V_{bb} + \frac{1}{CR_s}V_c \\ \frac{dV_c}{dt} & = \frac{1}{C_{bb}R_s}V_{bb} - \frac{1}{C_{bb}R_s}V_c - \frac{1}{C_{bb}R_p}V_c. \end{cases} \tag{4.10}$$

The system will exhibit a sliding motion if $s\dot{s} < 0$. Once the following condition $s\dot{s}$ is met, the system will demonstrate a sliding motion. Then, the sliding surface's derivation:

$$\dot{s} = \frac{dI_L}{dt} = \frac{V_{bb}}{L} - \frac{V_{dc}}{2L} - \frac{V_{dc}}{2L}\text{sign}(s) \tag{4.11}$$

Invoking control action (4.2), the condition $s\dot{s}$ can be defined as

$$s\dot{s} = \frac{1}{L}\left(-(\frac{V_{dc}}{2} - V_{bb})s - \frac{V_{dc}}{2}|s|\right) < 0 \tag{4.12}$$

Consequently, depending on the sign of the sliding surface, two attraction domain conditions can be obtained from (4.12) as

$$V_{dc} > V_{bb}, \tag{4.13}$$

$$V_{bb} > 0. \tag{4.14}$$

When the source voltage V_{dc} exceeds the capacitor voltage V_{bb}, the system motion is drawn to the sliding surface.

Using control scheme (4.2) and after solving $\dot{s} = \dfrac{dI_L}{dt} = 0$, the equivalent control $u_{2_{eq}}$ can be defined as

$$u_{2_{eq}} = 1 - \frac{V_{bb}}{V_{dc}} \tag{4.15}$$

Furthermore, the following dynamic equations investigate the system's stability during step-up operation under a sliding manifold.

$$\frac{dI_L}{dt} = 0 \tag{4.16}$$

$$\frac{dV_{bb}}{dt} = -\frac{(1-u_{1_{eq}})}{C}I_{\text{ref}} - \frac{1}{CR_s}V_{bb} + \frac{1}{CR_s}V_c \tag{4.17}$$

$$\frac{dV_c}{dt} = \frac{1}{C_{bb}R_s}V_{bb} - \frac{1}{C_{bb}R_s}V_c - \frac{1}{C_{bb}R_p}V_c \tag{4.18}$$

The above equations represent a second-order system. Invoking sliding-mode current control, which regulates I_L, leads to an order reduction. Thus, using (4.17)-(4.18), one can defined the following characteristic polynomial

$$P_{su} = \frac{-1}{CC_{bb}R_sR_p}\left(\lambda^2 CC_{bb}R_sR_p + \lambda(CR_p + CR_s + C_{bb}R_p) + 1\right). \tag{4.19}$$

The investigated P_{su} (characteristic polynomial) verifies the system's stability if both R_s and R_p are positive. This criterion will always be met during the step-up mode and its stability.

4.5.4 Voltage Control Loop Design

The bidirectional converter's voltage control loop, also known as slow dynamics, was neglected in the previous stability analysis. The effects of current reference variations have been considered when regulating the PI controller's voltage. The voltage control loop is incorporated into the proposed sliding surface as follows:

$$s = I_L - K_1(V_{\text{ref}} - V_c) - K_2\int(V_{\text{ref}} - V_c)dt \tag{4.20}$$

With consideration towards the low-frequency hypothesis, the sliding surface equation (4.20) has been given as follows:

$$s = I_L - I_{\text{ref}} \tag{4.21}$$

where

$$I_{\text{ref}} = K_1(V_{\text{ref}} - V_c) + K_2\int(V_{\text{ref}} - V_c)dt. \tag{4.22}$$

Invoking the condition (4.23), the equivalent control (4.24) can be determined as

$$\frac{ds}{dt}\,|_{u=u_{eq}} = 0, \tag{4.23}$$

$$u_{eq} = \frac{L\frac{dI_{\text{ref}}}{dt} - V_{bb}}{V_{dc}} + 1. \tag{4.24}$$

The converters with the SMC use the dynamic equations for law demonstrated in (4.16)-(4.18), even though the corresponding control is defined by (4.24) because

the current reference's dynamics are considered. By analysing the expression of V_{bb} from (4.18), and using (4.24), one can write (4.17) as follows:

$$C_{bb}R_s\frac{d^2V_c}{dt} + \frac{dV_c}{dt} + \frac{R_s}{R_p}\frac{dV_c}{dt} = \frac{-L}{CV_{dc}}\frac{dI_{\text{ref}}}{dt}I_{\text{ref}} + \frac{1}{CV_{dc}}I_{\text{ref}} - \frac{C_{bb}}{C}\frac{dV_c}{dt} - \frac{1}{CR_p}V_c. \tag{4.25}$$

According to (4.25), transfer functions of the poles are on the left side of the s-plane, which ensures stable performance of the voltage controller in the step-up mode.

Using the same procedure as described in (4.23)-(4.25), we can determine the ratio of Laplace transform of the reference current I_{ref} to output voltage V_c and the step-down mode's transfer function can be expressed as follows:

$$\frac{V_c}{I_{\text{ref}}} = \frac{-\frac{L}{CV_{dc}}sI^*_{\text{ref}}}{\left(C_{bb}R_s s^2 + as + b\right)V_c^*} \tag{4.26}$$

where $a = 1 + \frac{R_s}{R_p} + \frac{C_{bb}}{C}$ and $b = \frac{1}{CC_{bb}R_s}(\frac{1}{R_s} + \frac{1}{R_p})$

From (4.26), it can be noticed that the transfer function poles are on the left-hand side of the s-plane, ensuring stable voltage controller operation during the step-down mode.

4.6 Simulation Results

The designed controllers have been successfully implemented and validated using the MATLAB/Simulink environment. The system's parameters includes as follows: $C = 700\ \mu F, L = 5\ mH, R_s = 0.06\ \Omega, R_p = 1\ K\Omega, V_{dc} = 400V$. In (4.22), the current gain are chosen $K_1 = 10$ and $K_2 = 5$.

4.6.1 Simulations for G2V mode

The goal of the above section is to demonstrate the responses of the designed controllers in G2V mode. Fig. 4.9(b) illustrates the battery voltage V_{bb} to the reference voltage, V_{ref} of $230V$. which demonstrates the designed controller's successful implementation and performance. Similarly, Fig. 4.9(a) depicts the tracking current of

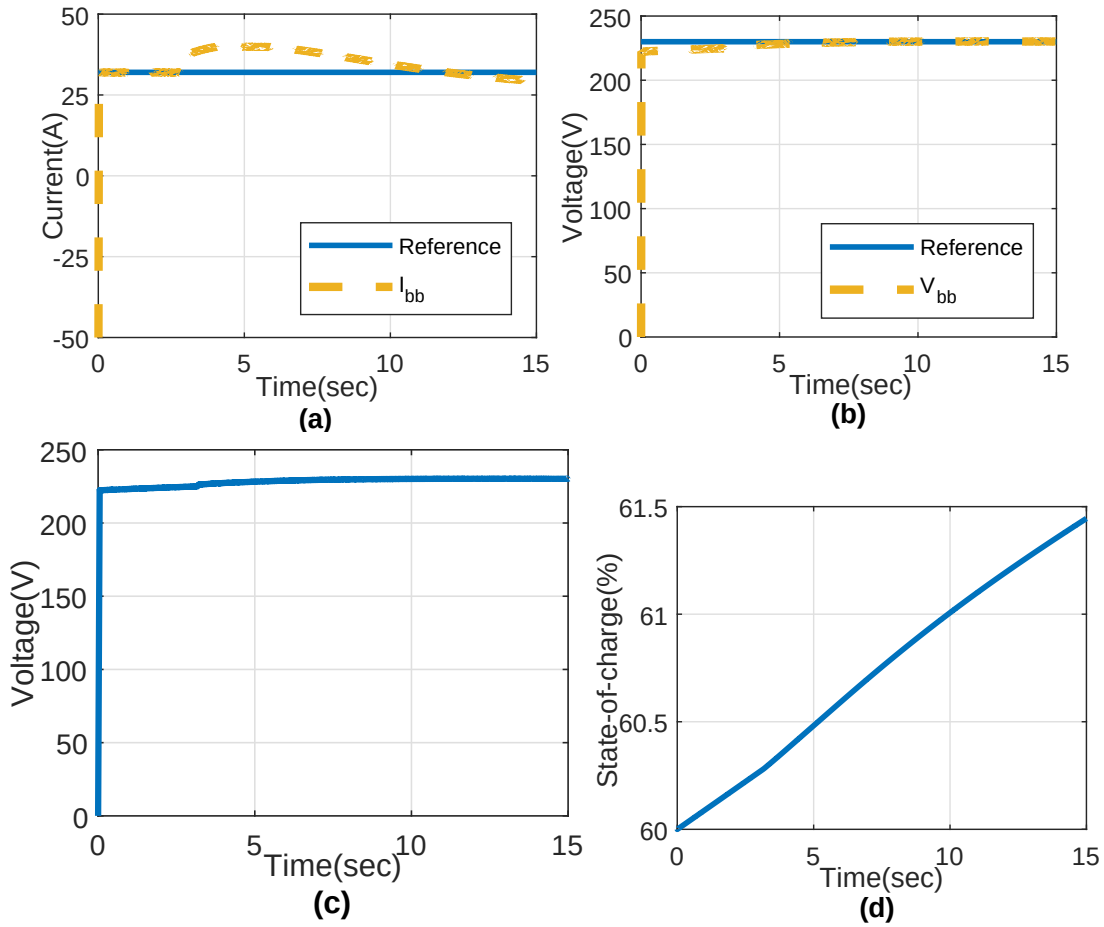

Figure 4.9: Charging phenomenon in G2V operation mode: (a) Battery current I_{bb}; (b) Battery voltage V_{bb}; (c) Battery inside voltage V_c; (d) State-of-charge.

the battery up to the $32A$ reference value of current. Fig. 4.9(c) depicts the inside voltage of a battery V_c. Fig. 4.9(d) displays the battery's state-of-charge (SoC).

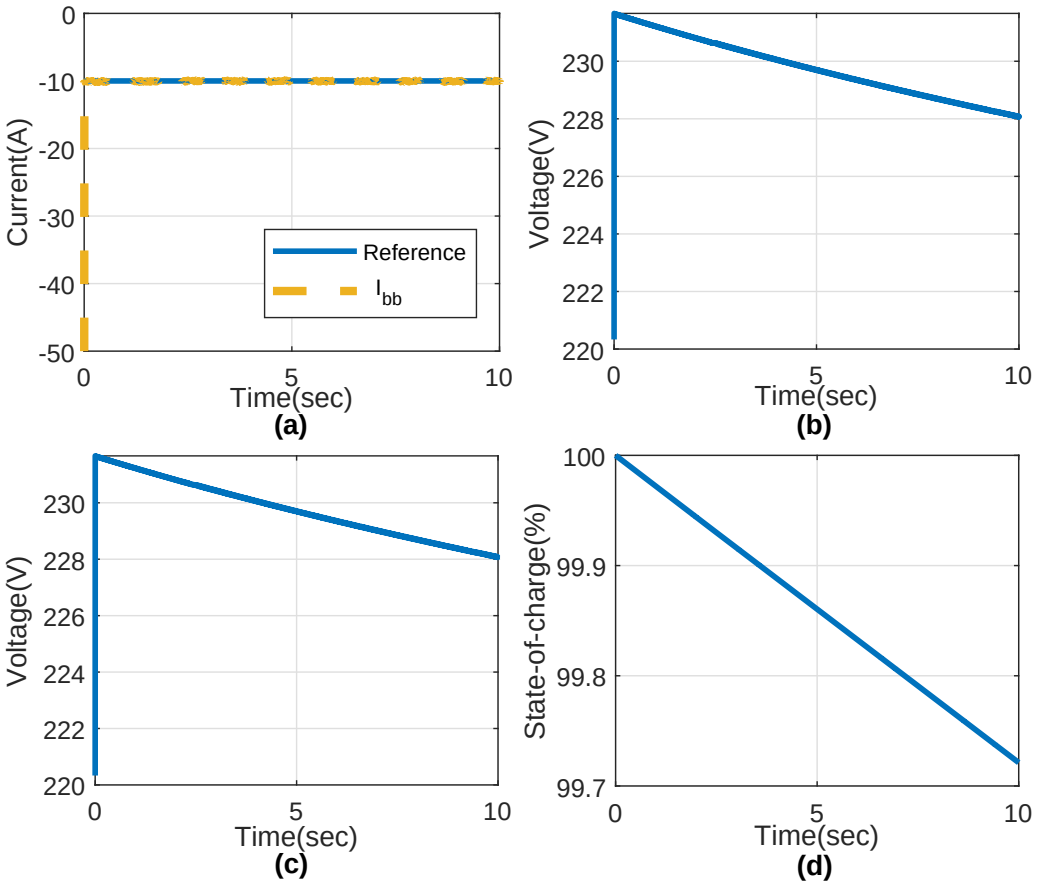

Figure 4.10: Discharging phenomenon in V2G operation mode: (a) Battery current I_{bb}; (b) Battery voltage V_{bb}; (c) Battery inside voltage V_c; (d) State-of-charge.

4.6.2 Simulation results for V2G Mode

This section illustrates how the designed controllers perform in V2G mode. Fig. 4.10(a) demonstrates the discharge of the battery with a negative reference of $10A$, and the designed control system successfully tracks the desired reference accurately. Figs. 4.10(b) and 4.10 (c) illustrate the discharging of the battery as a result of decreases in battery voltage. Based on Fig. 4.10(d), we can conclude that the SoC of the battery is not rapidly degrading, and the fast draining of the battery is preserved. In current work, conducted detailed simulations and experimental tests to verify the proposed SMC strategy for the bidirectional DC-DC converter used in electric vehicle chargers. However, additional case studies with varied operating conditions and real-world implementations would provide even more comprehensive validation. Future work will focus on expanding experimental testing to evaluate long-term

performance, robustness against parameter variations, and real-time implementation challenges.

.

4.6.3 Potential limitations of SMC-Chattering Issue:

To explore potential limitations of SMC, particularly the issue of chattering, in this chapter has implemented boundary layer techniques and higher-order sliding mode control to mitigate chattering, as acknowledge that practical applications may still face challenges in high-frequency switching scenarios. Future extensions of this work will investigate more advanced control strategies, such as adaptive SMC, Super twisting SMC (ST-SMC) and continuous control approaches, to further reduce chattering effects while maintaining system stability and efficiency.

4.7 Summary

The battery electric vehicle charger provides a highly effective bidirectional interface for G2V and V2G modes, facilitating efficient charging and discharging of the battery. This work investigated the utilization of a sliding mode controller for the control of BEV chargers in both G2V and V2G operations. The implementation of the sliding mode control in this converter guarantees unconditional stability during the sliding motion for both step-up and step-down modes, removing the requirement for the converter to identify its operating mode. A significant drawback of SMC is the chattering phenomenon, characterized by high-frequency oscillations that can lead to mechanical wear and increased energy losses. The chattering effect is a serious issue in power converters, mitigated by the super-twisting algorithm in the next chapter's proposed controller. To address the slower dynamics of the output voltage, the stability of the converter was initially established for the current control loop, followed by the construction of the voltage control loop in a cascaded manner. Simulation results substantiated the efficacy of the proposed controller in achieving the desired control objectives.